

SSC19-V-06

INSPIRESat-1: An Ionosphere and Solar X-ray Observing Microsat

Spencer Boyajian, Bennet Schwab, and Amal Chandran
Laboratory for Atmospheric and Space Physics, University of Colorado Boulder
1234 Innovation Drive, Boulder, CO 80303; 813-334-4770
Spencer.Boyajian@lasp.colorado.edu

Ankit Verma, Priyadarshan Hari, Anant Kumar, KVLN Malikarjun
Indian Institute of Space Science and Technology
Valiamala Road, Valiamala, Thiruvananthapuram, Kerala 695547, India; 91-471-256-8452
ankit.sc15b075@ug.iist.ac.in

Yi Duann, Loren Chang, Chi-Kuang Chao, Rong Tsai-Lin, Tzu-Ya Tai, Wei-Hao Luo, Chi-Ting Liao,
Chieh-Ju Chung, Ru Duann
Center for Astronautical Physics and Engineering, Institute of Space Science, National Central University
No. 300, Zhongda Road, Zhongli District, Taoyuan City, Taiwan 320; 866-3-422-7151
cntwtpe@g.ncu.edu.tw

ABSTRACT

The International Satellite Program in Research and Education's (INSPIRE) first satellite is an Ionosphere and Solar X-ray observing microsat slated for launch in November of 2019 onboard an ISRO Polar Satellite Launch Vehicle. The microsat has a mission specific structure fitting on a PSLV ring deployer. There are two payloads aboard with two different science objectives. The Compact Ionosphere Probe (CIP) will take in-situ measurements of ion density, composition, temperature, velocity, and electron temperature. The CIP is a smaller version of the Advanced Ionosphere Probe (AIP, both developed in Taiwan) currently operating onboard the FORMOSat-5. This instrument is capable of sampling the ionosphere at 1 and 8 Hz. The second payload is the Dual Aperture X-ray Solar spectrometer (DAXSS). DAXSS is a modified Amptek X123 that will observe Solar X-rays, specifically soft X-rays. Hot plasma in the sun's corona is best measured in the soft X-rays. Many emission lines for important elements (Fe, Si, Mg, S, etc) are in the soft X-ray range. Soft X-rays are always present in the sun but 100 times brighter during flares, these observations will also lend to understanding the temperature difference between the sun's corona and photosphere. The solar soft x-rays are also important for the Earth's Ionosphere, adding to the ionosphere observations made by CIP. The DAXSS instrument has heritage from a NASA calibration rocket experiment and two cubesats, MINXSS 1 and 2. The newer model Amptek X123 has much improved energy resolution for the X-ray spectrum. The primary science objectives of the INSPIRESat-1 are twofold. First, enabling the characterization of the temporal and spatial distributions of small-scale plasma irregularities like plasma bubbles and the Midnight Temperature Maximum (MTM) in season, location, and time by CIP. Second, giving a greater understanding of why the Sun's corona is orders of magnitude hotter than the photosphere, why there is an abundance of elements change during different solar events, and how these events (observed with greater soft x-ray fidelity) effect the earth's ionosphere. In this paper, we present science expectations for the INSPIRESat-1 and a concept for coordinated Ionospheric measurements covering several altitudes and local times using three satellite platforms carrying the same CIP instrument (INSPIRESat-1, IDEASat/INSPIRESat-2, INSPIRESat-4, FORMOSat-5). We describe the development of DAXSS and how the dual aperture prevents the need for two X123 to get the similar data. We also highlight the unique development of the INSPIRESat-1 microsat being developed by international collaboration across three different universities.

INTRODUCTION

The International Satellite Program in Research and Education's first satellite (INSPIRESat-1) is a custom-built small satellite weighing ~ 8.6 kg with dimensions of 290x200x160 mm (~ 9U), slated for launch in December 2019. It is aimed to study ionosphere, its ion composition, plasma densities, ion velocities, and ion temperature. Furthermore, it will observe Solar X-rays that will help shed light on the temperature difference between the Sun's Corona and Photosphere. The focus of Compact Ionospheric Probe (CIP) data collection is on eclipse time and the transition time from sunlight to eclipse time while that of The Dual Aperture X-ray Solar Spectrometer (DAXSS) is at sunlight side. The design, realization, and operation of the INSPIRESat-1 aims to combine the expertise of the participating institutions to enable science and give real-world engineering experience to student participants. The INSPIRESat-1 spacecraft contains the inhouse developed CIP, and DAXSS as the payloads, Command and Data Handling (C&DH), Electrical Power Supply (EPS), off the shelf Blue Canyon Technology's (BCT) XACT as Attitude Determination and Control System (ADCS), SpaceQuest's TRX-U Ultra High Frequency (UHF) transceiver, and Cape Peninsula University of Technology's STX as S-Band transmitter. The student developed C&DH and EPS systems are expected to be utilized in the future satellites developed by the INSPIRE program.

PAYLOAD – CIP

The CIP, developed by Space Payload Laboratory at NCU, was selected as a science payload in the 1st International Satellite Program in Research and Education (INSPIRE) Workshop held at NCU in 2016. The CIP, a successor of Advanced Ionospheric Probe¹, is an all-in-one plasma sensor that uses a single instrument to perform multiple sensor functions in a time-sharing mechanism.

It performs in-situ measurements of the ionospheric plasma compositions, ion concentrations, velocities, and temperatures to explore the terrestrial ionosphere.

The data collected by the CIP will give insight to ionospheric phenomena like plasma bubbles and mid-night temperature maxima. The plasma bubbles can cause scintillation in the GPS signals. The ion density will identify the plasma bubbles since the satellite will pass through these bubbles at some angle which will be indicated by the sudden drop in the ion density measurement of the CIP. The Figure 1 shows the

plasma bubbles identified by the data collected by the Ion Velocity Meter (IVM) instrument.⁶

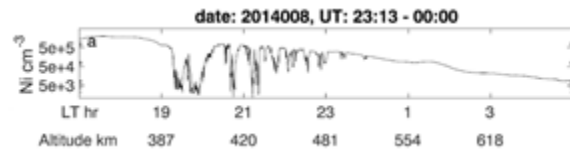


Figure 1: Plasma Bubbles Identified in C/NOFS Data

The Figure 2 shows the mechanical structure of the CIP.

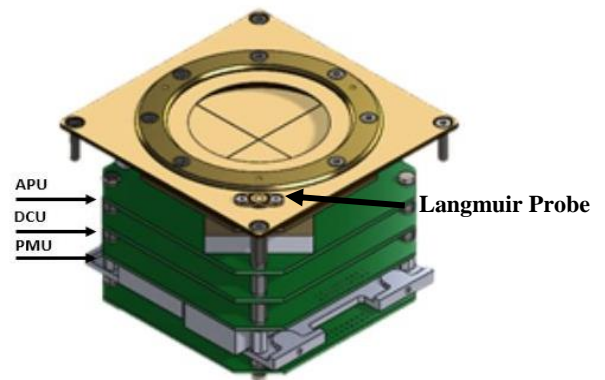


Figure 2: CIP mechanical structure

The CIP contains three circuit boards:

1. Analog Preprocessing Unit (APU): It transduces currents from the sensor into digital signals.
2. Digital Control Unit (DCU): It controls digital to analog/analog to digital converters (DA/ADs) on APU board, monitors PCBs' temperature, and receives commands/sends science data from/to C&DH.
3. Power Management Unit (PMU): It supplies and regulates necessary powers for CIP.

Table 1: Preliminary CIP specifications

Parameters	Value
Mass	0.5 Kg (< 1 Kg)
Dimension	0.7 U
Voltage	12 V
Power	3.45 W
Interface	UART, 115200 bps (RS422)
Connector	9-pin D-sub female.

The preliminary specifications of the CIP are present in Table 1. The data is transferred to the C&DH using UART over RS422 lines. The C&DH communicates

with the CIP at 115,200 ±1% baud, with 1 start bit, 8 data bits, and one stop bit.

Modes of Operation

CIP has the following operation modes:

1. Planar Langmuir Probe (PLP): Measures electron temperature.
2. Ion Drift Meter (IDM)/Ion Trap (IT): Provides arrival angles of ion velocity and ion density.
3. Retarding Potential Analyzer (RPA): Measures ion temperature, ion composition, ion density and ion ram velocity.

Each mode can either be in normal mode or fast mode. There is one data packet available every second in normal mode and 8 every second in fast mode.

The C&DH formats CIP commands into 8 bytes consisting of 2 header bytes, 1 function code byte, 4 data bytes (time tag or command), and a checksum byte computed using 3rd through the 7th command bytes. The CIP will reject commands with bad framing or checksum. The C&DH sends all commands to the CIP within the 900 ms interval of one of the one second (1PPS) pulses, as shown in Figure 3:

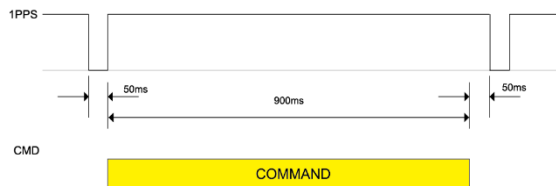


Figure 3: Command synchronization with the PPS signal.

Two kinds of science data packets are available. One is the raw science data packet (280 bytes) and the other is processed science data packet (60 bytes). The CIP raw science data packets are 280 bytes long. Each packet shall start with a 23-byte header that consist of 2 start bytes, 1 function code byte, 4-byte data time tag, and 16-byte status of health (SOH) data. The header will be followed by 256-bytes of CIP science data. The data will be followed by one-byte checksum. The checksum byte shall be constructed using the 3rd byte through the 279th byte of this data packet. The processed science data consists of 23 bytes header, 36 bytes of science data (processed) and 1 byte of checksum constructed using the 3rd byte through the 59th byte.

CIP shall transmit all data packets within the period starting at the leading edge of the C&DH PPS signal

and ending at least one-half period before the following PPS.

PAYLOAD – DAXSS

The DAXSS payload is comprised of an X-ray Spectrometer, a Solar Position Sensor (SPS), a small Solar Irradiance Measurement instrument (PicoSIM), a CDH board, an EPS board, and an interface board. The X-ray spectrometer is the commercial off the shelf (COTS) Amptek X123 Fast Silicon Drift Detector (SDD) with Si-PIN detector and beryllium filter which can detect Soft X-ray (SXR) photons with energies between 0.5-30keV with better than 0.15keV energy resolution. The SPS/PicoSIM package is designed in-house and the SPS can achieve solar pointing knowledge of a few arc-seconds with an 8-degree field of view. All flight boards are designed in-house and both the CDH and EPS boards have flight heritage on both of the MinXSS-1 and MinXSS-2 satellites.

The SXR regime measurable by DAXSS is desirable for solar physicists studying the sun. Soft X-rays are constantly emitted by the sun but can be up to 100 times brighter during solar flares. The motivation behind looking at this portion of the solar spectrum is that it may be used to better model and predict atmospheric heating and expansion, satellite drag, communication blackouts, power grid failure, and spikes in harmful radiation. The sun's continuum is observable between 0.5-30keV and furthermore there are many emission lines which can be used to identify the relative abundances of elements present in the sun. By combining DAXSS spectra with solar-atomic databases such as CHIANTI^{7,8}, a model can be formed to calculate the temperature and emission measure of the sun at the time of observation. Through comparing the intensity of emission lines, the first ionization potential (FIP) factor or relative abundance of elements in the sun can further be added to the model. With the data collected by DAXSS the scientific community moves closer to obtaining answers to important questions such as why is the temperature of the sun's corona orders of magnitude hotter than its photosphere? And why do the abundances of elements change during different solar events?

DAXSS is a continuation of the three science instruments that flew on the MinXSS-1 CubeSat² in 2016-2017 and the MinXSS-2 CubeSat⁴ in 2018-2019. The exact instruments of DAXSS were flown and recovered from a June 2018 sounding rocket flight and provided the highest resolution X-ray solar spectrum from an X123 instrument and has enabled

identification of many more elements in the solar SXR spectrum⁵.

One significant improvement of the X-ray spectrometer of DAXSS over that of the MinXSS satellites is in its dual aperture design. This novel design, shown in Figure 4 incorporates a thin Kapton filter to attenuate lower energy photons between 0.5-2keV while allowing higher energy photons between 2-30keV to penetrate through. The dual aperture enables detection of higher energy photons in greater numbers without saturating the instrument with a large amount of low energy photons. As a result, greater spectral resolution across a wider energy range is captured.

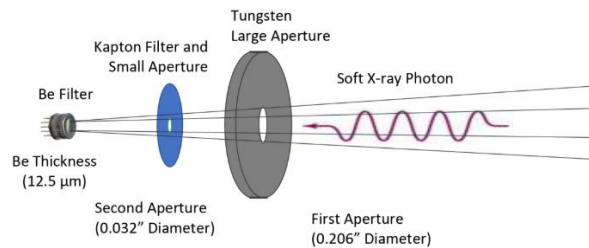


Figure 4: The dual aperture design of DAXSS showing the two apertures, the Kapton filter, and the Beryllium filter of the X123 X-ray spectrometer.

The dimensions of the DAXSS electronics assembly, including the X123 Electronics, CDH, EPS, and interface board are 100x130x83mm, slightly larger than a 1U form factor. The SPS and PicoSIM are packaged together in a 70x38x22mm box. The X123 Sensor dimensions with its housing are 47x28x29mm. The CDH of INSPIRESat-1 is the master processor in a master-slave relationship with the CDH of DAXSS. The master has the ability to turn on and off power to the DAXSS payload as a whole or commands from the master CDH can be sent to DAXSS to individually. Examples of such commands could be to turn on and off the instruments or to change various table parameters of DAXSS.

MISSION DESIGN

The science aim of the mission is twofold. First is to use CIP to study the ion composition, ion densities, ion velocities, and ion temperature of the ionosphere at mid altitude regions and secondly use DAXSS to measure the soft X-ray (SXR) spectrum of the sun during a quiescent period through solar maximum. With this data we can study solar flares, solar cycles, and try to understand the process of the sun's coronal heating. Beside the scientific aim, the goal of the

mission is to develop a small spacecraft by collaboration among different institutes all around the world. The mission statement is as follows:

Improve the understanding of Ionosphere dynamics through observations of ion temperature, composition, density and velocity. Improve our understanding of the sun's coronal heating processes by measuring the Soft X-Ray spectrum of the sun.

Orbit Details

To make mid-latitude nighttime ionosphere measurements to study ionospheric effects of mid night temperature maxima and nighttime Ionospheric plasma bubbles, INSPIRESat-1 desired orbit requirements are:

1. Altitude: 500 ± 50 km
2. Inclination: $55^\circ \pm 10^\circ$

This gives us orbital period of ~ 95 minutes with 35-minutes average eclipse times. The 60 minutes of sunlit time would allow the DAXSS to take readings of the soft X-ray spectrum of the sun.

Design

To meet the mission requirements each subsystem has been either developed in-house or commercially procured. The Table 2 gives the details of each subsystem:

Table 2: Subsystem and responsible institute

Subsystem	Short Description	Institute
Payload	Compact Ionosphere Payload (CIP)	NCU
	DAXSS	LASP
C&DH	Self - developed	IIST
Power	Self - developed	IIST, NCU
Structure and Thermals	Self - developed	LASP
ADCS	XACT, Blue Canyon Technology	LASP
Communication	TRXU - Space Quest, STX - Clyde Space	NCU

BCT XACT is highly capable ADCS system. Power subsystem is designed to provide stable and adequate power to all subsystems. Communication subsystem incorporates UHF transceiver - TRXU from SpaceQuest and S-Band Transmitter - STX from Clyde Space. C&DH has been developed to incorporate all the interfaces, controlling them and data storage of at least 3 months. Structure has been developed based on ISRO launch loads, strong enough to survive launch and space environments.

For interconnection between subsystems standard PC104 is used. The commercial off the shelf components have a nano/micro-D type connector that is re-routed to PC104 connectors through an interface card. The Figure 5 shows the placement of each subsystem in the structure:

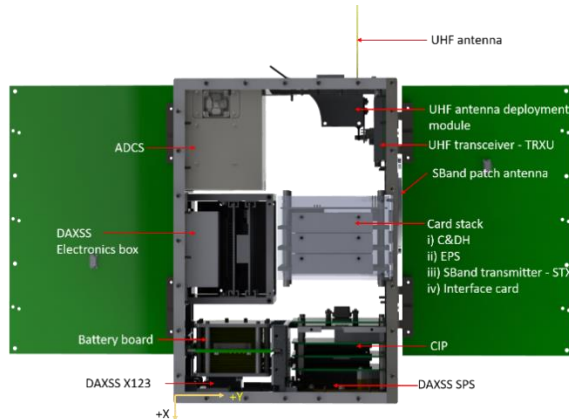


Figure 5: INSPIRESat-1 internal structure and Co-ordinate axis

Analysis

Access Time and Downlink

The Figure 6 shows the access time for the three ground stations of INSPIRESat-1.

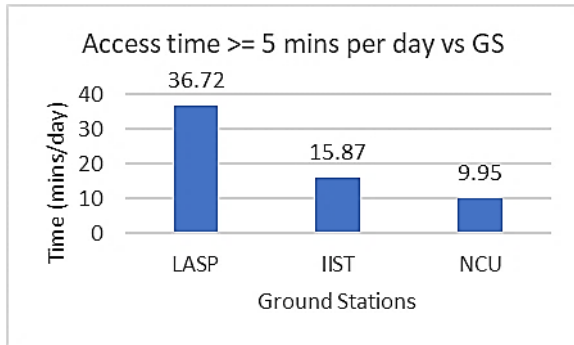


Figure 6: Access time

The data is downlinked over SBand frequency at the data rate of 2×10^6 bits per second (bps) to LASP while the uplink and downlink over UHF band at 9600 bps. Other ground stations will use UHF for the uplink and downlink of essential HK data. The Table 3 give the number of megabits can be downlinked over different ground station.

Table 3: Downlink data per day

GS	Access time per day (minutes)	UHF data (Mb/day)	SBand Data (Mb/Day)
LASP	36.72	-	4202.27
IIST	15.87	8.72	-
NCU	9.85	5.41	-
Total	62.54	14.13	4202.27

Power Analysis

The power analysis has been done to find out the power generation and hence prepare a power budget. The concept of the power analysis is as follows:

1. Satellite's +X (Figure 5) points in direction of velocity during eclipse time for payload to take reading.
2. Satellite's solar panels point in sun direction during sunlit period.
3. A buffer of 5 minutes is provided for satellite at the start and end of eclipse to switch from RAM orientation to sun pointing, during this time sunlight falls at an angle on the solar panels, which is obtained from System Took Kit (STK).
4. Solar panels are operating with an efficiency of 26.6% at 65° C (worst case).
5. Buck converters are extracts power from the solar panels with 90% efficiency.
6. Satellite does not produce any power during S-Band transmission. Since S-Band patch antenna is +Y face of the satellite (Figure 5), it is assumed that no power is generated when the +Y of the spacecraft is pointing towards the nadir direction as a worst-case scenario.

Following are the solar panel inputs:

1. No. of solar cells: 30
2. Area of each cell: 30.84 cm²

The analysis of power generation has been done in the time interval of 1 year, from September 1, 2019 to September 1, 2020.

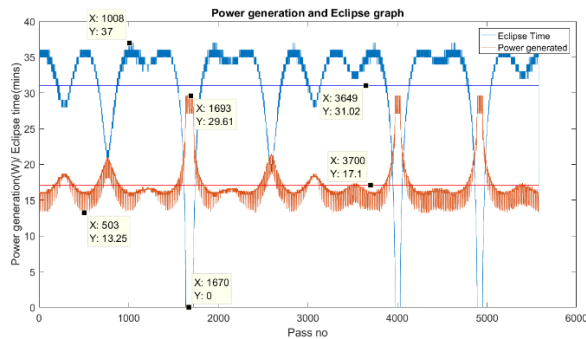


Figure 7: Power Generation over 1 year

The Figure 7 shows the power generation profile in one orbit over the span of 1 year along with the eclipse time.

Table 4: Power Budget

Subsystem	Peak Power (W)	Nominal Power (W)	Duty Cycle (%)	Average Peak power (W)	Average Nominal power (W)
C&DH	1.40	0.91	100	1.40	0.91
DAXS	5.2	3.5	50	2.6	1.75
Power	1.78	1.78	100	1.78	1.78
ADCS	2.82	2.82	100	2.82	2.82
GPS	1.70	1.50	100	1.70	1.50
CIP	5.00	3.47	50	3.07*	2.30*
TRXU RX	0.25	0.25	100	0.25	0.25
TRXU TX	8.00	6.50	9.62	0.77	0.63
STX TX	5.00	5.00	2.55	0.13	0.13
Battery Heater	4.64	4.64	1.00	0.05	0.05
			Total	14.57	12.12
			Power Gen	17.10	17.10
			Margin	17.36%	41.09%

The average power generated = 17.10 W with maximum instantaneous power of 29.61 W. The power budget has been made based on average power consumption in an orbit by all the subsystems as shown in Table 4.

*CIP standby power consumption = 1.14 W.
For CIP Avg power = Duty_Cycle * Peak_Power(or

$$\text{Nominal_Power} / 100 + (1 - \text{Duty_Cycle} / 100) * \text{Standby_Power}.$$

Modes of Operation

The modes of operation have been divided into 5 modes based on battery's State of Charge (SOC) and payload operation as shown in Table 5.

Table 5: Modes of Operation configuration

Subsystem	Phoenix	Safe	Charging	Science	
				SciC	SciD
CDH, EPS, TRXU RX	ON				
ADCS	OFF	Coarse Sun pointing	Fine sun pointing	Fine ref in RA M direction	Fine sun pointing
CIP	OFF			ON	OFF
DAXSS	OFF			ON	
TRXU TX	As required				
STX TX	As required				
Battery Heater	As required				

The CDH and EPS subsystems are always ON since they are the basic subsystems of the satellite. The TRXU is ON and by default configured in receive mode. In safe mode ADCS points the solar panels towards the sun with no constrain on any other axis this is coarse sun pointing of the ADCS. In charging and SciD mode ADCS points the solar panels towards the sun with constrain +Y of the spacecraft pointing as close as possible towards the nadir direction. In SciC mode the ADCS points +X of the spacecraft towards the velocity direction with +Y of the spacecraft pointing as close as possible towards nadir direction. The Phoenix and Safe modes' purpose are to increase the SOC of the battery and hence together are called emergency modes. The Charging and Science modes of operation together are called normal modes. The Figure 8 shows the mode flow followed by the spacecraft.

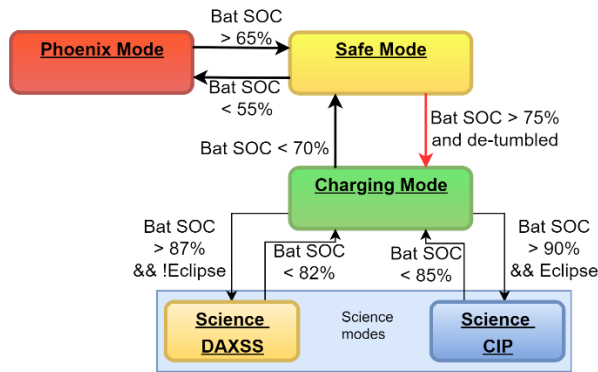


Figure 8: Mode flow diagram

Mode oscillations are avoided by providing two thresholds values between any two modes which introduces hysteresis. The mode flow, Figure 8, along with the mode profile, Table 5, shows that as the satellite progress from phoenix mode to the science modes the complexity of the system increases step wise.

COMMAND AND DATA HANDLING (C&DH)

C&DH uses System On Module (SOM) provided by Emcraft. The SOM uses a System On Chip (SOC) provided by Microsemi. The SOC contains a microprocessor embedded in a Field Programmable Gate Array (FPGA). The off the shelf SOM is integrated with the rest of the satellite by a ‘C&DH card’. The C&DH card contains PC104 to interface with other subsystems.

The C&DH is responsible for collecting House Keeping (HK) data from all subsystems and science data from the payloads. It configures subsystems and maintains a Real Time Counter (RTC) for time tagging the data and scheduling the tasks. The FPGA is used to implement more interfaces, which are controlled by microcontroller via an Advanced High-Performance Peripheral Bus (AHPB).

Electrical characteristics:

The Table 6 gives electrical details of C&DH:

Table 6: Electrical characteristics of C&DH

Sr. no.	Parameter	Value
1.	Voltage	3.3 ± 0.3 V
2.	Peak Power	1.40 W
3.	Nominal Power	0.91 W
4.	Operating Temp	-40° C to 85° C

The CDH consumes 1.4 W when the processor is running at its full potential of 166 MHz and FPGA is

more than 80% utilized. In practice, we will be using 60 MHz for the processor and FPGA will be less than 50% utilized.

System On Module (SOM)

SOM is an off the shelf module from Emcraft. It contains a 12 MHz quartz crystal and other clocks are derived from it by using PLLs present in SOM. It contains:

1. 32-Bit Arm Cortex-M3 processor.
2. 64KB embedded SRAM (eSRAM).
3. 512 KB embedded NVM (eNVM).

Interface Definitions

The Table 7 gives the interfaces of the C&DH with various subsystems.

Table 7: Interfaces definitions

Subsystem	Interfaces
CIP	UART – RS422 (x1); CIP PPS – RS422 (x1)
ADCS	UART – RS422 (x1)
EPS	I ² C (x3); PWM (x3); Distribution control lines (x5); Deployment control lines (x3)
TRXU	UART (x1); GPIO lines (x6)
S-Band	I ² C (x1); SPI (x1); GPIO (x2)

The C&DH card

The fabricated C&DH card is shown in Figure 9.



Figure 9: Command & Data Handling: Top view

1. The lines for RS422 and TRXU GPIO lines pass through bus transceiver to protect the SOM from fluctuations in voltage and current. The bus transceiver also corrects the logic level to 3.3 V and 0 V for logic level 1 and 0 respectively.

- Four RS422 Converter ICs converts UART for CIP and ADCS, and PPS line to RS422 for CIP.
- The flight board contains two SD Cards slots on single SPI bus. Using two provides redundancy if one of them fails.
- A reset IC that contains a watchdog timer is connected to the SOM module, providing the first level of reset. It is also a clock input to a 4-bit counter that counts the number of reset from reset IC to microprocessor. If the count value goes to 8 (b'1000) then the signal for External System Reset to the EPS board. EPS cuts the power supply to all subsystems and turns the power supply ON back with a delay of 1 sec.

INTERFACE CARD

Interface card is responsible for connecting various subsystems to the PC104 stack of C&DH, EPS and STX transmitter. The Figure 10 shows the fabricated interface card.

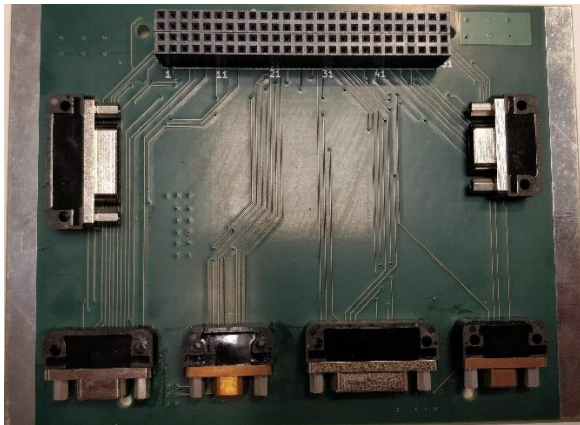


Figure 10: Interface card: Top view

It contains military grade (MIL-DTL-M83513) connectors for ADCS & GPS, TRXU, CIP, DAXSS and GSE have been provided in the interface card.

FLIGHT SOFTWARE

The flight software of INSPIRESat-1 is a non-interrupt software with no operating system. It is basically an infinite loop performing different tasks. Lack of interrupt and scheduler introduces challenges like timing constraints, tasks priority etc. Hence the FPGA is used to parallelize several I/O tasks which traditionally is handled by the μ P using interrupts. This not only frees up the microprocessor's resources but also provides a memory space for buffering the data coming at I/Os by using the block RAMs of the FPGA.

Since the architecture is free of interrupts, the possibility of false interrupt has been ruled out. The software provides Failure Detection, Recovery and Isolation (FDRI) which detects the failure of a subsystem to communicate with the C&DH, take some measures to reset the subsystem and if all fail then isolate the subsystem by avoiding mode.

The tasks which need the bit level of operations like AX.25 protocol etc. have been offloaded to the FPGA where it is easy to do bit operations. Following I/O and bit level tasks have been implemented on the FPGA

- UARTs each with buffer of size 8192 bytes (8KB)
- PPS generation for the CIP.
- Scrambling and descrambling of the data received by the radio over UHF band.
- NRZI encoding and decoding of the data received by the TRXU transceiver.
- High level Data Link Control (HDLC) frame formation and Frame Check Sum (FCS) calculation.
- I2C modules.
- Two real time counters, one for scheduling various tasks while the other for keeping track of the UTC time for timestamps.

Architecture

The Figure 11 shows the architecture of the flight software developed for the INSPIRESat-1.

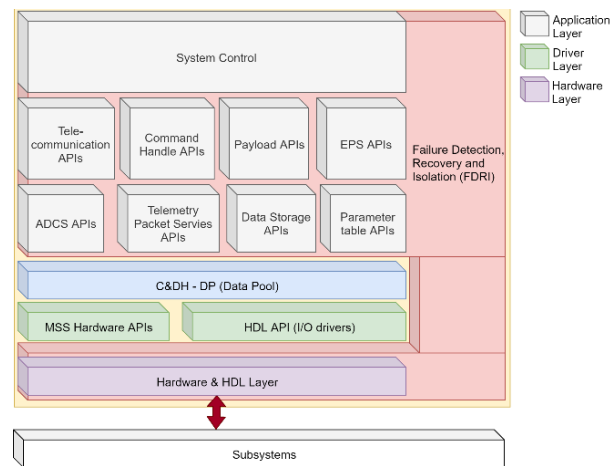


Figure 11: Top-level architecture

The architecture of the software has been divided into three layers with hardware layer at the bottom followed by the driver layer with application layer at the top.

At the bottom of the architecture the Hardware & Hardware Descriptive Language (HDL) layer is present which directly communicates with different subsystems over the physical layer. This layer consists of different in-house developed Verilog modules and modules which are hard coded in the FPGA like GPIOs, SPI etc. They receive & store and transmit data from & to subsystems and modules like SD card, SPI flash etc.

The next layer is called the Driver Layer because it consists of APIs which are required for μP to communicate and control various Hardware Description language (HDL) modules present in the Hardware & HDL layer. The modules present in this layer allow the microprocessor to read and write from and to the buffers available in the FPGA and control the modules to communicate with different subsystems.

The C&DH - Data Poll layer represents all the global variables and is shared among various modules of the application layer only. The data is not shared by the Driver layer. The Application Programming Interface (API) of application layer communicate with the Hardware layer via Driver layer and share the obtained data with other APIs of the application layer if required.

The Application Layer consists of modules for various subsystems and tasks related to different modules of the C&DH like flash memory, SD card, etc. The System control modules uses various application layer modules to carry out mission operations. The application layer together with the hardware & HDL layer provides the FDRI capability, with hardware & HDL layer providing the failure detection functionality while recovery and isolation is provided by the application layer.

ELECTRICAL POWER SUPPLY

The Electrical and Power System (EPS) of a spacecraft is a very vital and critical subsystem that is expected to provide sufficient and regulated power for the operation of the entire spacecraft. The Figure 12 shows the fabricated EPS board.

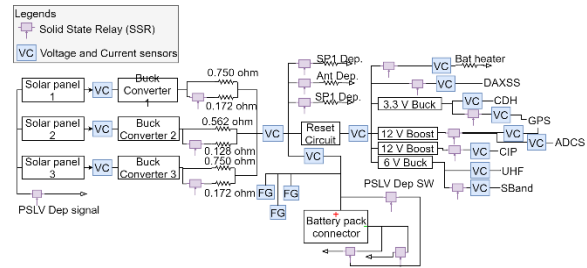


Figure 12: EPS architecture

1. The EPS is designed to accept power from 3 solar panels each with independent buck converters.
2. Mechanical relay is used as reset switch which on getting the signal from C&DH cuts off the battery from bus and then connects it back to the bus after a delay of approximately 1 second.
3. 2 DC-DC synchronous step down (buck) converters and 2 DC-DC synchronous step up (boost) converters are provided in the design on load side to cater to voltage requirements of the loads.
4. The EPS features 2 critical I²C buses and a non-critical I²C bus on which the various VC (Voltage Current) sensors and one Analog –Digital Converter (ADC) are placed on different I2C lines.
5. VC sensors are placed to measure voltage across and current through the followings:
 - a. Solar panels and bus voltage & current.
 - b. Subsystems: CIP, CDH, ADCS, GPS (12 V and 3.3V), Comm (TRXU and STX) and DAXSS
 - c. Battery and battery heater.
6. Triple Modular Redundancy with Majority Voting Logic (MVL) is used for fuel gauge.

Solar cells and Panels

AzurSpace 3G30C solar cells have been chosen for the mission because of their heritage on the MinXSS² mission. The characteristics of the solar cells are listed in Table 7:

Table 7: Solar cell characteristics

Sr. No.	Parameter	Value
1	Cell Volume	30.18 cm ³
2	Peak power voltage	2.411 V
3	Efficiency at 25°C	29.5%
4	Peak Power current	0.5044 A
5	Bypass diode	Yes

INSPIRESAT-1 has 3 panels for solar cells, one body mounted with 12 cells, and two deployable panels with 9 cells each.

Battery Pack

Table 8: Battery Characteristics

Sr. No.	Parameter	Value
1	Nominal Voltage	3.7V
2	Nominal Capacity	2000 mAh/ 7.4 Whr
3	Dimension	60 x 54 x 5.8 mm
4	Charge cut-off voltage	4.2 V
5	Operation Temperature	-20 °C to 60° C

A 2S-3P configuration of Sparkfun Polymer Lithium-Ion Batteries are selected to meet the load requirements of the mission because of their heritage on the MinXSS² mission. The battery characteristics are listed in Table 8.

EPS interfaces

The EPS has three I²C interfaces that are connected to the voltage current and temperature sensors on the board. The distribution of critical sensors has been done among the 3 I²C lines to have triple redundancy. The two components that have been identified as critical are Voltage and Current sensor (VC sensor) for solar panels and fuel gauge. In addition, GPIO lines from the CDH provide to control the distribution of power among various subsystems.

COMMUNICATION

The communication sub-system receives and transmits data between the INSPIRESat-1 and ground. The spacecraft COMM and ground-station shall allow a data-rate of 193.5 MB/day during fast mode of CIP (payload), and 24.18 MB/day during normal mode.

SpaceQuest TRX-U transceiver

The layout and connector identification of TRX-U is indicated in the 13. J2 is RF output connector, and the transmit power is 2 Watts. J1 contains all the interfaces to C&DH and power.

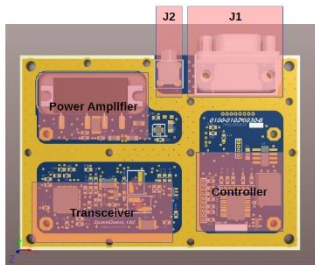


Figure 13: Layout and Connector Identification of TRX-U.

CPUT STX transmitter

CPUT STX is with a CubeSat Kit PC/104 form factor, and the modulation of it is QPSK. The data rate is up to 2 Mbps.

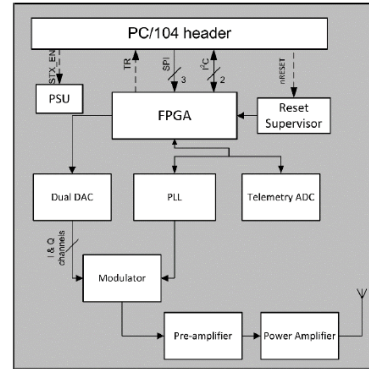


Figure 14: Block diagram of the CSK header connections. Broken lines indicate optional connections.

The only non-optional connection to the header (excluding power signals) I²C and SPI interface fits our Flight software FPGA well. (Figure 14) All signal voltage levels are 3.0 V LVCMOS. A 50 Ω SMA connector will be used for transmitting RF.

Antenna for UHF and S-band

The UHF band uses the tape antenna and tests are being carried out at present.

The CPUT SANT S-band patch antenna has been selected to be used for high data rate communication with INSPIRESat-1. The antenna offers a default left hand circular polarization with a moderate gain of 8 dBi max. The frequency of operation is in the amateur band of the S-band frequency range (2.4 - 2.5 GHz). It is interfaced with the satellite through an SMA connector and weighs around 50gms. The dimensions of the antenna are 89 mm x 81.5 mm x 4.1 mm. The S11 10 dB bandwidth is around 90 MHz.

UHF Link Budget³

Table 9: Data parameters for calculation of TRXU subsystem

Bit Error Rate / Probability of Bit Error	1E-5	[-]
Data Coding Scheme	GMSK /GFSK	
Required Bit Energy to Noise Ratio	9.6	dB
Data Rate	9600	bps (Hz)
Carrier to Noise Ratio Density	49.42	dB-Hz
Required Design Margin	3.00	dB

Minimum Pr/No	52.42	dB-Hz
---------------	-------	-------

The basic parameters of our mission for calculating link budget are discussed in this section. (Table 9.) Maximum and minimum are defined by different transmitting power. The orbital parameters in link budget follow the mission design. SpaceQuest TRX-U module is selected as our UHF transceiver. We are using 437 MHz. The elevation angle is 10° limited by the NCU ground station. Pass duration is about 7 minutes, and the data transfer per pass (full duplex) is 132 kB.

For the transmitter, Uplink represents our ground station and Downlink represents the TRXU module on the satellite.

As for receivers, Uplink is for the TRXU module on the satellite and Downlink represents the ground station. Notice that there is an amplifier in the ground station (Downlink only), so we got more Receive Antenna Gain here.

Table 10: UHF subsystem link budget

Link Budget	Uplink		Downlink		Units
	MAX	MIN	MAX	MIN	
Propagation Losses	-152.9	-152.9	-152.93	-152.9	dB
Receive System Gain	1.00	1.00	30.92	30.9	dB
Received Power	-123.7	-135.7	-118.25	-119.5	dBW
Receiver Sensitivity	-141.0	-141.0	-152.00	-152.0	[-]
Power Margin	17.34	5.30	33.75	32.50	dBW
System Noise Power	-200.4	-200.4	-199.1	-199.1	dBW/Hz
Carrier to Noise Ratio Density	76.7	64.66	80.84	79.59	dB-Hz
Minimum Pr/No	52.42	52.42	52.42	52.42	dB-Hz
Link Margin	24.28	12.24	28.42	27.17	dB

The Table 10 shows us the quality of UHF communication in our mission. The estimating table shows us that we have positive link and power margin in the interval of maximum and minimum transmitting power, which means we will have a condition of communication that is good enough for the mission.

S-band Link Budget

The S-band transmitter is the Cape Peninsula University of Technology (CPUT) STX. The frequency is set as 2.402 GHz according to the capability of ground station at LASP in Boulder. The data parameters of S-band subsystem is shown in Table 11. The data rate is 2.0×10^6 bps (Hz), and the data transfer per pass (full duplex) is 27530 kB. Other system parameters are the same as in UHF calculations.

Table 11: Data parameters for calculation of S-band subsystem

Bit Error Rate / Probability of Bit Error	1E-5	[-]
Data Coding Scheme	QPSK	
Required Bit Energy to Noise Ratio	9.6	dB
Data Rate	2000000	bps (Hz)
Carrier to Noise Ratio Density	72.61	dB-Hz
Required Design Margin	3.00	dB
Minimum Pr/No	75.61	dB-Hz

We follow the specification of ISIS ground station. Receiver System Amplifier Gain is based on the datasheet of Transcom low noise amplifier.

Table 12: S-band link budget

Link Budget	MAX	MIN	Units
Propagation Losses	-167.91	-167.73	dB
Receive System Gain	69.35	69.35	dB
Received Power	-90.84	-99.08	dBW
Receiver Sensitivity	-152.00	-152.00	
Power Margin	61.16	52.92	
System Noise Power	-196.87	-196.87	dBW/Hz
Carrier to Noise Ratio Density	106.03	97.79	dB-Hz
Minimum Pr/No	77.91	77.91	dB-Hz
Link Margin	28.12	19.88	dB

As the result indicated in Table 12, after applying amplifier, the link margin is *positive*.

ATTITUDE DETERMINATION AND CONTROL

The ADCS sub-system for the INSPIRESat-1 has been procured from Blue Canyon Technology based out of Boulder, Colorado. The XACT is capable of 0.003° pointing accuracy in two axes and 0.007° in the third axis, which far exceeds the requirement of 5° in all three axes for the INSPIRESat-1 mission. The XACT has flight heritage on several small spacecraft missions

including the successful MinXSS-1 mission developed at LASP at CU Boulder. The BCT XACT occupies 0.5U plus an additional 0.1U for the GPS receiver and has an approximate mass of 887g (excluding sun sensors and GPS). The XACT will communicate with C&DH over an RS-422. The XACT requires 12V lines from the EPS fed to the reaction wheels and to the XACT bus.



Figure 15: BCT XACT

The XACT has two modes of operation: Sun Point and Fine Reference Point. Sun point is the XACT safe mode that operates using a minimal sensor suite to point the sun sensor of the spacecraft towards the sun. Fine reference point uses the entire sensor suite available to the XACT (including GPS) to provide high precision pointing to any vector necessary. The XACT needs to be able to point the spacecraft -Z face to the sun during sun-lit portions of the orbit, point the +X face in the ram direction during eclipse, and maintain these orientations while experiencing disturbance torques.

STRUCTURE

The design of INSPIRESat-1's structure, heavily driven by the need to use ISRO's IWL-150 Deployer, has one face completely free of components except for deployment switches. This side will be removable to allow easier installation of the satellite's components during assembly. The fore-end ring will be attached to the bottom faceplate of the satellite via 6 M5x0.8 screws and remain with the microsat post-separation from the launch vehicle. The structure will be fabricated from aluminum 6061-T6. INSPIRESat-1 will use hinges and antenna deployment module (ADM) developed and flown by MinXSS to attach and deploy the solar panels and UHF respectively. Additionally, card rails will be used to hold the battery pack assembly, and card stack in place. The main board stack comprised of EPS, CDH, interface card, and the S-Band radio card, slide into 3 pairs of Kooler card rails attached within the avionics mounting structure. All other components directly attach to the structure. Locking HeliCoil inserts are used in almost all connections to ensure screws do not back out during launch. Most of the microsat is held

together with #4-40 socket head cap screws, torqued to spec using a torque screwdriver. The cable routing was kept as simple as possible, allowing easier assembly.

Below is the fully assembled CAD model and distinctive views followed by the results of the finite-element-analysis (FEA) of stresses induced by launch. Much care and detail must be put into preparing FEA as the conditions must be closely simulated for the results to have significance. For example, bolts were modeled by calculating the resulting pressure cone area and mating those two areas between parts. This allows the observation of how the plates will flex and bend while still attached to one another. Furthermore, the mesh generated must be evaluated to ensure good approximations. This was done by using ANSYS' element quality read out available after generation, then tuning the mesh control parameters. Elements from the mesh are used to approximate a finite region of the material, turning it into a tetrahedral shape with equations defining its sides as springs. The more accurately you fit these tetrahedral shapes within the material, the more accurate the results from the FEA. It is the main goal of the analysis to prove the structure shall not endure any plastic deformations, stresses higher than components are rated for, or failures.

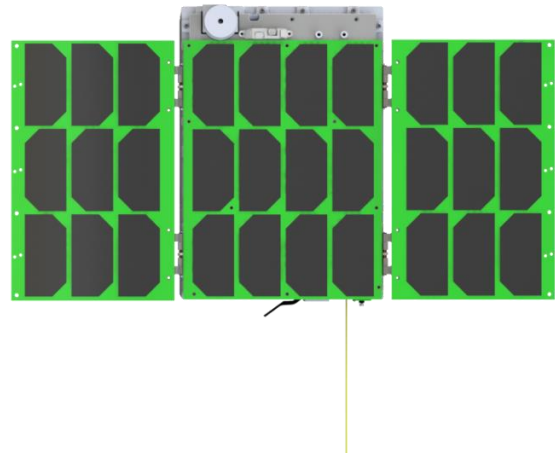


Figure 16: The solar panel side of INSPIRESat-1

The layout of INSPIRESat-1's externally visible components are shown in Figure 16 and 17.

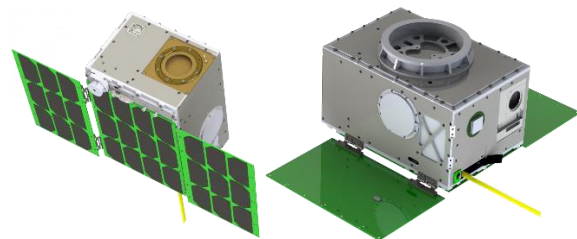


Figure 17: INSPIRESat-1 ISO views.

Testing all launch orientations possible, we found that when loaded through the y axis, the highest stresses occur. They fall well within the capabilities of the materials: Aluminum 6061.

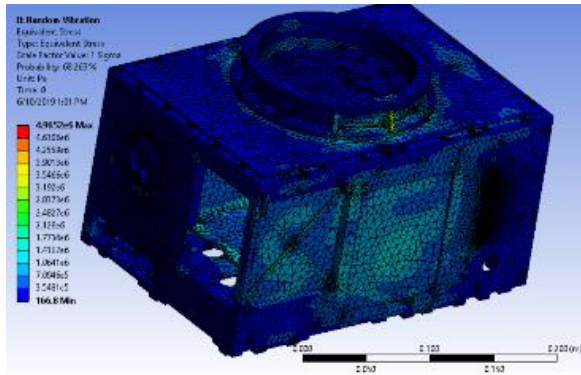


Figure 18: Equivalent stress from FEA of worst-case vibration

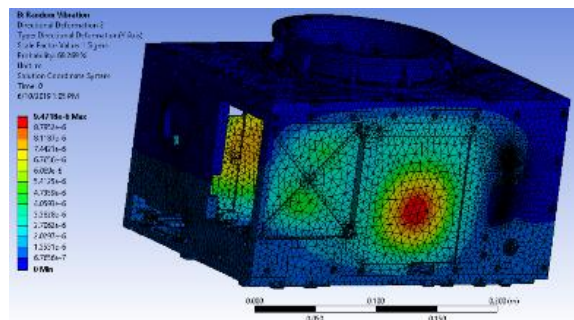


Figure 19: Y axis deformation from FEA of worst-case vibration

Above shows the equivalent stress (Figure 18) and deformation in the Y axis (Figure 19) when the worst-case vibrational loads are applied. Results show that the structure has survived an extreme case of loading comparable to almost 3 times that which it is expected to experience. In fact, the minimum factor of safety throughout these scenarios remains above 2.48. This was achieved after many revisions and weight-relieving efforts. The total mass of INSPIRESat-1 is 8.6705 kg including harnessing, with the structure being less than half that.

THERMAL

The thermal subsystem of the INSPIRESat-1 is responsible for maintaining the temperature of all of the components. The operating temperature range of CIP and the X123 detector will drive the need for passive thermal control. To remain operational, CIP

must remain between -10°C and +50 °C. The X123 detector has a Thermo-Electric-Cooler (TEC) to maintain optimal temperatures, dumping heat to the spacecraft structure. It has been determined that a structure temperature ranging from 10°C to 30°C will provide ample temperature differential for the TEC to sink heat to. Additionally, the thermal subsystem must be able to cope with worst-case conditions. These being when the satellite is in eclipse in it's the lowest possible beta angle orbit (cold case), or sunlight in the highest beta angle scenario (hot case). To evaluate Nominal, worst-case cold, and worst-case hot scenarios, a simulation was created in AutoCAD using a thermal software called Thermal Desktop by CR Technologies.

Simulating all methods of attachment, conductance, emissivity, and other material properties. The accuracy of the results is similar to FEA in that the setup defines the significance. It is very important to match your part weights with the weights assigned by density in Thermal Desktop. Errors in mass directly cause errors in total heat capacity, undesirably. The software allows for surface coatings and multi-layer-insulation (MLI) to be simulated increasing fidelity and confidence in the performance of specialized surfaces. Creating the orbit and programming the attitude of the satellite throughout is essential for accuracy as well. This attitude will determine the heating rates through the specified orbit positions. Again, modeling the bolts and their conductance's' produced increases the significance of the results. When dealing with detectors and cooling in space one must very accurately determine the conductance's' around it to have confidence in the results. Even just a small change in the conductance can yield greatly different detector temperatures. As with battery packs, thermal isolation is key.

For the hot case, the orbit orientation is varied to produce the most sun-lit orbit we will experience with an inclination of 55 degrees. This occurs when the orbits beta angle is maximum. The beta angle is the angle between the sun vector and orbit normal. Additionally, all loads are simulated to run at their respective peak power values. Only, exception being peak power values that occur for less than half a minute. Several methods of heat transfer are in play and were accounted for and modeled properly in the analysis to ensure accuracy.

- Solar Radiation (Flux) Incident on the Spacecraft = 1.412 kW/m² in early January to 1.321 kW/m² in early July

- Earth Albedo (Flux) Incident on the Spacecraft = 0.4236 to 0.3963 kW/m²
- Earth IR Radiation = Spacecraft and Earth's average temperature of 15°C radiation (Black body to Sat)
- Radiation to Space environment = -270.45 °C (2.7K)
- Internal Radiation = radiation between the internal surfaces of the spacecraft
- Conduction = Heat's movement through the solid/contacting parts of the spacecraft
- Internal Heat Generation = Heat generated by the electrical components of the spacecraft

These loads were applied accordingly, and the different materials of the model specified. This includes thermal conductivity, absorptivity, and emissivity. The emissivity of materials can be changed with coatings such that it can be used as a tuning knob for the thermal design. For example, the solar facing side of the X123 sensor head has silver faced Teflon tape to reduce solar heat influx. An additional copper thermal strap is utilized for moving heat from the S-Band radio card to the structure. Results from Thermal Desktop in Figure 20 and 21 show the temperature of the spacecraft in nominal operations shortly before it enters eclipse. The solar panels get the hottest, approximately 75°C while the structure averages 21°C. The solar panels are unsurprisingly hot as well as the regions around the electronics during the hot case.

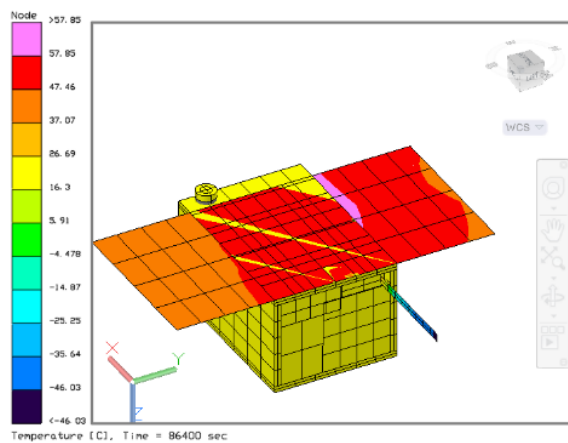


Figure 20: Spacecraft temperatures halfway through the sunlit portion of the orbit

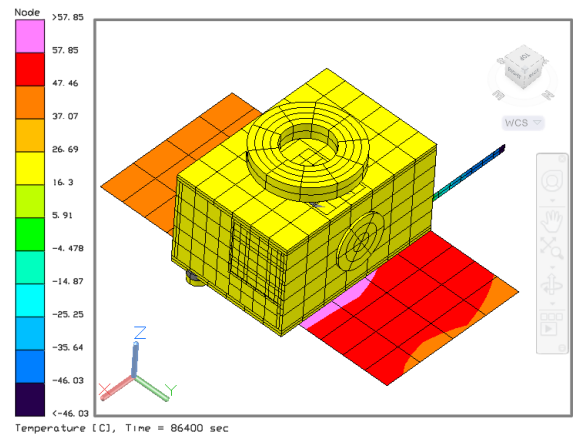


Figure 21: Spacecraft temperatures halfway through the sunlit portion of the orbit

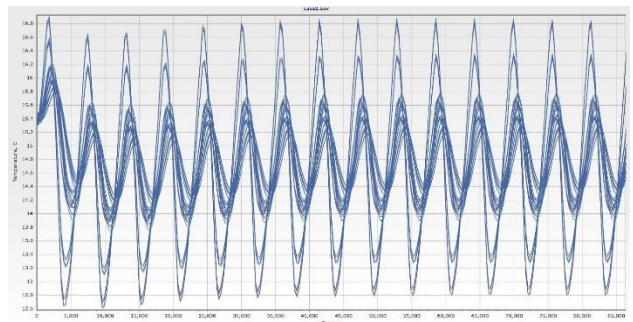


Figure 22: Spacecraft battery pack temperature

CIP experiences temperatures between 22°C and 40°C, well within its operational temperature. The battery pack has heaters set to turn on at 5°C and turn off at 10°C however in nominal operations it was found that they should not be needed (Figure 22). This is by design, thermally isolating the battery back to contain all heat and minimize the power needed for the heaters. The simulations for the worst-case hot nominal, and worst-case cold scenarios have shown that all thermal constraints and limits for operation put forth by components are satisfied. With the exception of the X123 detector and solar panels, components stay within the desired range or temperatures for operations, -10°C to 50°C. This range was set by CIP as it has the narrowest operational limits. The avionics and other components have ranges wider than this, solar panels with the largest.

TESTING

Flatsat testing

The flatsat testing is scheduled to be performed to qualify the in-house developed C&DH, EPS and the flight software for the mission. The testing includes

interfacing various subsystems with the C&DH & EPS and verifying the operations of the subsystems. The flatsat testing will commence once the interfaces of all the subsystems have been fabricated. The flatsat testing will be an end to end testing with data being collected from various subsystems and stored in the SD card and transmitted to the ground station when commanded by it. Command execution tests have already been performed and the results have been verified. Long range communication test, across half the city of boulder, is essential to testing satellite communications before launch. This simulates ground to satellite operation. Additionally, day-in-the-life testing reveals expected battery state of charge values useful for determining duty cycles of instruments.

Thermal vac test

Before going into the thermal vacuum (TVAC) chamber, the spacecraft components are first sonic cleaned and put into a bake out test (BOT) chamber. In BOT, the spacecraft is brought to 60 degrees Celsius under vacuum and left to dwell for over 24 hours. A residual gas analysis test is done on the contents of the chamber to ensure the cleanliness of the spacecraft. Once complete, the spacecraft is bolted down to the platen of the TVAC chamber and thermistors are adhered to its sides. A solar array simulator (SAS) is connected to the inputs of the solar panels on the spacecraft so that power may be applied as if the solar panels were experiencing sunlight. The current and voltage curves of the SAS are controlled via a MATLAB script to replicate what may be expected on orbit, complete with periods of “sunlight” and periods of “eclipse”.

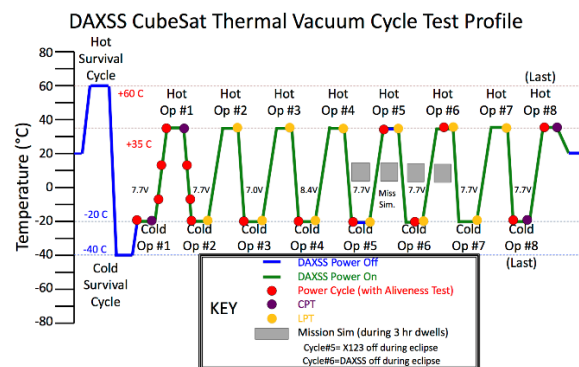


Figure 23: The temperature profile of thermal vacuum (TVAC) testing.

The two main goals of thermal cycling are to ensure nominal, functional operation over the predicted temperature ranges the system will experience on orbit and to stress test the system over 8 thermal cycles to

provide workmanship qualification. The TVAC procedure follows the trend shown in Figure 23. With the spacecraft powered off, its temperature is brought to the limits of survival hot (60 °C) then survival cold (-40 °C) and left to dwell for 4 hours at each survival extreme. The survival temperature values were determined for each subsystem by the component within the subsystem with the tightest temperature constraints while powered off. These temperature ranges for are shown in Table 13 along with the operational ranges found by the component per subsystem with the tightest temperature constraints while powered on and operational.

Table 13: DAXSS Subsystem Operational and Survival Temperature Range Requirements

Subsystem	Operating Range [°C]	Survival Range [°C]
CDH, EPS, SPS, I/F	[-30, +70]	[-40, +85]
X123 detector	[-20, +40]	[-60, +60]
X123 electronics	[-20, +50]	[-40, +85]

Once the spacecraft returns to -20 °C after the cold survival cycle, the spacecraft is turned on and an aliveness test is performed to briefly check the health status of each subsystem. The thermistors integrated in each subsystem are used to track their internal temperatures. For each hot (35°C) or cold (-20°C) operational dwell, these internal temperatures are maintained within 3°C from the target temperature and the duration of each dwell lasting for one hour. Near the middle or end of each dwell, either a Comprehensive Performance Test (CPT) or a Limited Performance Test (LPT) will be performed to test the status of each subsystem in depth and to test the execution of all possible commands. During the first operational cycle the spacecraft is turned off and on to simulate the spacecraft turning on at various on-orbit temperatures. Eight operational thermal cycles are completed, and any anomalous behavior is logged and followed up on during a post-TVAC meeting.

Vibration test

The spacecraft must undergo stresses associated with launch aboard a Polar Satellite Launch Vehicle (PSLV). After simulating these launch loads, the assembled spacecraft is attached to a baseplate, vibrate fixture, which attaches to the vibration test machine. This test verifies that the structure can survive vibrational loading. After the launch’s vibration

profile is applied, a visual inspection of all components is completed. Then a comprehensive performance test is performed to ensure all components remain operational. The testing of the deployment mechanisms is extremely important at this stage, helping to verify that the deployment methods are robust enough to function after launch.

CONCLUSION

The INSPIRESat-1 is being developed via an international collaboration not usually seen on this type of mission. The mission will measure properties of the Earth's ionosphere to better understand irregularities like plasma bubbles, the midnight temperature maximum, and characterize sun's soft X-Ray spectrum. This will lead to better understanding and prediction of how the ionosphere negatively affects GPS and also help explain the difference between the temperature of the sun's corona and photosphere. INSPIRESat-1 will be delivered to Indian Space Research Organization (ISRO) in October, pending launch in December. The next few key steps include hardware integration, flatsat tests, deployment tests, thermal vacuum, and vibration tests.

REFERENCES

1. Lin, Z. W. et al: "Advanced Ionospheric Probe scientific mission onboard FORMOSAT-5 satellite", 2017
2. Mason, J.P. et al, "Miniature X-Ray Solar Spectrometer: A Science-Oriented, University 3U CubeSat", *Journal of Spacecraft and Rockets*, Vol. 53, No. 2, pp. 328-339, doi: 10.2514/1.A33351, 2016
3. Brown, C.D., "AIAA Education Series: Elements of Spacecraft Design", American Institute of Aeronautics and Astronautics, Inc., pp 447 – 490, eISBN: 978-1-60086-179-6, doi: 10.2514/4.861796, January 2002.
4. Mason, J. P., T. N. Woods, P. C. Chamberlin, A. Jones, R. Kohnert, B. Schwab, R. Sewell, A. Caspi, C. S. Moore, S. Palo, S. C. Solomon, and H. Warren, MinXSS-2 CubeSat mission overview: Improvements from the successful MinXSS-1 mission, *Adv. Space Res.*, doi.org/10.1016/j.asr.2019.02.011, arXiv: 1905.01345v1, 2019.
5. Schwab, B et al, (2018, December). "Novel Dual Aperture Design for Soft X-ray Solar Spectrometer: Measurements from June 2018 Sounding Rocket". Abstract ID: 345468. AGU Fall Meeting 2018.
6. Evonosky, W et al, (2018 August), "INSPIRESat-1: An Ionosphere Exploring Microsat". SmallSat paper ID: SSC18-WKIV-04. SmallSat 2018
7. Dere, K.P., Landi, E., Mason, H.E., Monsignori Fossi, B.C., Young, P.R., 1997. CHIANTI – an atomic database for emission lines. *Astron. Astrophys. Suppl. Ser.* 125, 149– 173. URL: <http://www.edpsciences.org/10.1051/aas:1997368>, doi:10.1051/aas:1997368.
8. Landi, E., Del Zanna, G., Young, P.R., Dere, K.P., Mason, H.E., Landini, M., 2006. CHIANTI—An Atomic Database for Emission Lines. VII. New Data for X-Rays and Other Improvements. *As- trophys. J. Suppl. Ser.* 162 (1), 261–280. URL: <http://stacks.iop.org/0067-0049/162/i=1/a=261>, doi:10.1086/498148.
9. Moore, C. S., A. Caspi, T. N. Woods, P. C. Chamberlin, A. Jones, J. P. Mason, R. A. Schwartz, & A. K. Tolbert, The Instruments and Capabilities of the Miniature X-ray Solar Spectrometer (MinXSS) CubeSats, *Solar Physics*, **293**, A21, doi: 10.1007/s11207-018-1243-3, 2018.